Macroporous Structures

DOI: 10.1002/anie.200604143

Layer-by-Layer Constructed Macroporous Architectures**

Yujie Ma, Wen-Fei Dong, Mark A. Hempenius, Helmuth Möhwald, and G. Julius Vancso**

Macroporous materials (with pore sizes greater than 50 nm) present great application potentials,[1] however their preparation also poses fabrication challenges. To date, many approaches have been developed to produce films with high porosity, for example, colloidal templating, microphase separation of block copolymers, emulsion, casting, and leaching-out techniques.[1,2] An emerging approach encompasses construction of macroporous architectures by a "bottom-up" self-assembly approach using polyelectrolytes.[3]

Polyelectrolyte multilayers (PEMs), fabricated by electrostatic layer-by-layer (LBL) self-assembly, have seen tremendous progress in the last two decades.[4] Besides their versatility, ease of fabrication, and tuneable functionality, PEMs also offer the advantage of compatibility with functional species without loss of their specific functions.[5,6] Functional PEMs have potential applications in tuneable surface wettability, controlled drug release, and switchable permeability.[4,5] Herein we introduce a new PEM system consisting of two functional components, that is, high-molar-mass semiflexible double-stranded DNA and a flexible, strong polyelectrolyte, poly(ferrocenylsilane) (PFS; Scheme 1).[7c] Making use of the interplay of their specific molecular characteristics, we demonstrate the first layer-by-layer constructed macroporous architectures without using any further post-treatment following fabrication.[3] A main advantage of this strategy is that it could offer a universal and facile route to the fabrication of porous thin films containing other semiflexible polyelectrolytes, such as polysaccharides and liquid-crystalline (LC) materials. Moreover, water-soluble PFS polyelectrolytes[7] also belong to the class of stimuli-responsive materials. The redox-active component PFS[8,9] allows us to regulate the responsiveness of the films to, for example, chemical oxidation.[5]

The thin-film morphology was monitored by atomic force microscopy (AFM) in the tapping mode. After the deposition of a smooth, positively charged polyethyleneimine (PEI) layer (Figure 1a), the first DNA/PFS bilayer transforms the flat, featureless silicon surface to exhibit an irregular, weblike morphology (Figure 1b). This result is consistent with former reports on DNA network formation from solutions of relatively high concentrations.[10] The two-dimensional DNA network evolves with increasing the number of deposited polyelectrolyte layers into a three-dimensional hierarchical structure (Figure 1c and d). In this process, the surface roughness of the thin film increases with an increasing number of polyelectrolyte bilayers (Figure S1 in the Supporting Information). AFM images clearly show that the average pore size of the observed porous structure also increases with the number of bilayers, accompanied by an increase of the height of the ridges. Sectional analysis of a film consisting of ten bilayers (Figure 1d) exhibits sizes of the largest pores around 350 nm. These features make the as-formed structures macroporous.[1] The large-scale macroporous surface morphology was confirmed by scanning electron microscopy (SEM) imaging on the same type of samples (Figure 1e), and the pore sizes observed by SEM and AFM were similar. To preserve the features of the surface morphology no conductive layer was applied in SEM imaging, which limited the focal depth. Hence, the in-depth information about the macroporous morphology, which could be clearly observed in the AFM images, was somewhat compromised.

The film morphology peculiarly remains porous regardless of the choice of the last layer (DNA or PFS). This observation is in contrast with the layer-by-layer system consisting of DNA and other types of cationic polyelectrolytes, for example, poly(allylamine hydrochloride) (PAH). SEM images show a somewhat different appearance of surface morphology of (DNA/PAH) thin films with varying polyelectrolyte species as the outermost layer (Figure S2 in the Supporting Information). The difference in surface morphology when using PFS or PAH as the cationic polyelectrolyte species in the LBL process was considered to be the consequence of different hydrophobicity of the polycation backbone.

The formation of the peculiar porous structure is considered to result from an interplay of the persistence-length

[*] Prof. Dr. W.-F. Dong
Key Laboratory of Automobile Materials
Ministry of Education and Department of Materials Science and Engineering
Jilin University, Changchun, 130025 (China)
Fax: (+86) 431-509-5170
E-mail: wenfeidong@hotmail.com
Y. Ma, Dr. M. A. Hempenius, Prof. G. J. Vancso
Department of Materials Science and Technology of Polymers & MESA+ Institute for Nanotechnology
University of Twente
P. O. Box 217, 7500 AE Enschede (The Netherlands)
Fax: (+31) 53-489-3823
E-mail: g.j.vancso@tnw.utwente.nl
Prof. Dr. W.-F. Dong, Prof. H. Möhwald
Max Planck Institute of Colloids and Interfaces
14476 Golm/Potsdam (Germany)

[**] Y.M., M.A.H., and G.J.V. thank Mark A. Smithers (MESA+ Institute, University of Twente) for the SEM imaging, Jing Song and Anneliese Heilig (MPI-KG) for their help with the in situ AFM imaging. The University of Twente, the MESA+ Institute for Nanotechnology of the University of Twente, the Dutch Science Foundation for Chemical Research NWO-CW, and NanoImpuls, a Nanotechnology Program of the Ministry of Economic Affairs of the Netherlands are acknowledged for financial support. W.-F.D. and H.M. thank the Max Planck Society and the German Science Foundation (SFB 448) for financial support. W.-F.D. also acknowledges the support from Jilin University.

Supporting information for this article is available on the WWW under http://www.angewandte.org or from the author.

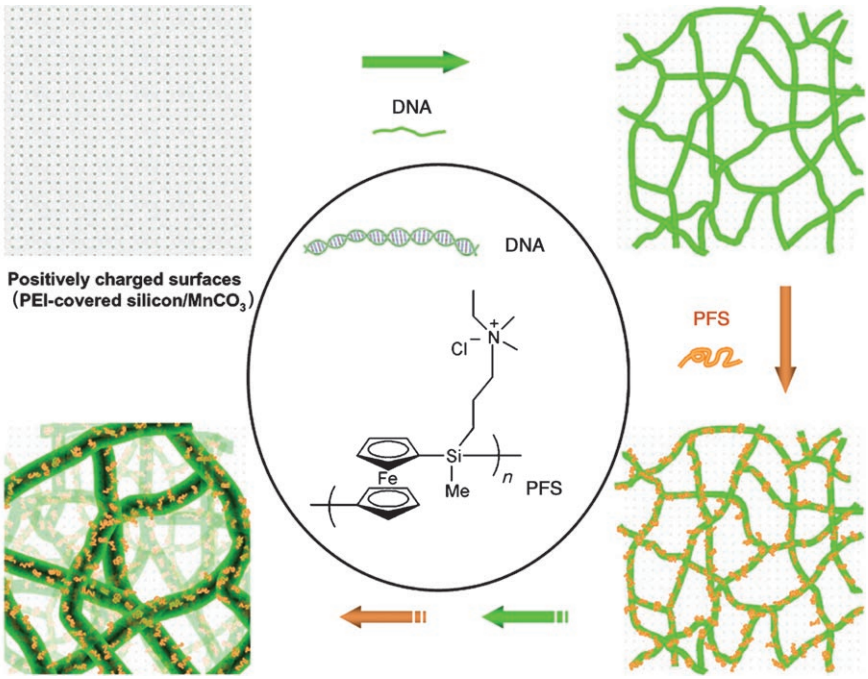

Scheme 1. Schematic of the preparation of macroporous DNA/PFS architectures by electrostatic layer-by-layer assembly. The semiflexible polyelectrolyte (DNA) forms a network onto which shorter and flexible PFS adsorbs, then the process is repeated to obtain a multilayer network. Chain lengths of PFS and DNA fiber diameters are approximately to scale.

much higher than that of PFS (5.3×10^4 g mol^{-1}). The molar-mass mismatch will in turn represent a difference in the size of the polymer coils upon their LBL deposition onto the substrates. Moreover, under the relatively high salt concentrations (0.5 M) of our experimental conditions, the charges on the flexible PFS (persistence length, $L_p \approx 1$ nm[11]) polycations will be completely shielded, forcing them to adopt a collapsed coiled conformation. In contrast, DNA is an extended anionic polyelectrolyte, with an L_p value of about 50 nm, which is relatively insensitive to ionic strength.[12] The large persistence length of DNA will tend to "direct" subsequent bilayer depositions, thus giving rise to an "aligned, bundle-like" structure.

To explain the formation and stability of the macroporous structures, the same type of $(DNA/PFS)_n$ multilayers (n represents the number of bilayers) were also fabricated without any drying steps in between layer-deposition steps. In situ AFM showed similar porous structures (Figure 2) when the samples were immersed in aqueous medium. The morphology observed did not depend on the choice of the last layer (Figure 2). These results indicate that the macropore formation may only marginally depend on the drying process, and a drying-induced phase separation was not the main driving force of structure formation. Thus, the as-formed hierarchical structures must originate from a rather equilibrated spontaneous assembly process. When aqueous solutions (NaCl, 0.5 M) of the two components were mixed, a water-insoluble complex was immediately formed, thus giving further support of the above explanation.

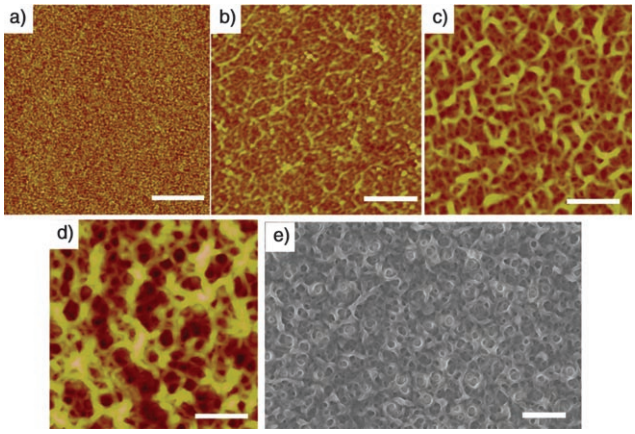

Figure 1. Tapping-mode (TM) AFM height images of silicon wafer with a) PEI layer; b) PEI + $(DNA/PFS)_1$; c) PEI + $(DNA/PFS)_5$; d) PEI + $(DNA/PFS)_{10}$. z range: 3.0 nm (a); 20 nm (b); 80 nm (c); 100 nm (d). Scale bar is 500 nm for (a)–(d). e) Top-view SEM image of a PEI + $(DNA/PFS)_{10}$ film on silicon surface; scale bar is 1 μm.

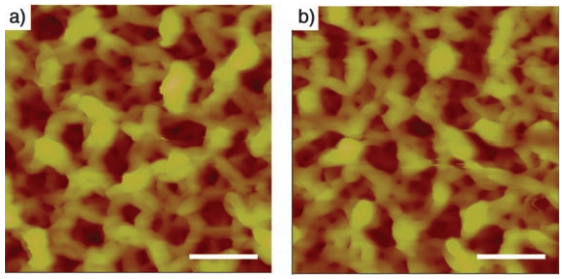

Figure 2. In situ TM-AFM images of a) PEI + $(DNA/PFS)_9$ + DNA and b) PEI + $(DNA/PFS)_{10}$ thin film on silicon substrates. Scale bar and z range are 500 nm for both images.

mismatch, chain-length/molar-mass mismatch, and the hydrophobic/hydrophilic nature of the two components. DNA molecules are hydrophobic/hydrophilic in nature because of the existence of hydrophobic bases and hydrophilic backbones that consist of repeating sugar molecules and phosphate groups. The PFS polycations have a very hydrophobic backbone and ionic hydrophilic side groups. The strongly hydrophobic PFS backbone is likely the cause of stable coordination with the DNA molecules. On the other hand, the DNA has a molar mass of about one million g mol^{-1}, which is

The pore-formation mechanism described above can be further confirmed and understood by studying the assembly, structure, and permeability of DNA/PFS microcapsules.

$(DNA/PFS)_5$ microcapsules were fabricated by LBL self-assembly onto positively charged manganese carbonate ($MnCO_3$) colloidal particles and subsequent template removal.[5] The self-assembly process was accompanied by severe aggregation, which was usually not observed for similar coatings made of common polyelectrolyte polyion pairs. Aggregation was observed earlier during the fabrication of other DNA-containing multilayer microcapsules, yet no clear explanation was given.[13] When SEM was used to visualize the dried templates with the multilayer coatings, thick bundles acting as "bridges" between the coated templates were observed (Figure S3 in the Supporting Information). These bundles, likely to be mainly composed of DNA, were considered to originate from the very large length of the DNA molecules (several μm). Apart from the apparent "bridging" effect, aggregation should also result from the electrostatic adhesion between the uncovered (that is, exposed) positively charged $MnCO_3$ surface and negatively charged DNA molecules.

After template removal, $(DNA/PFS)_5$ microcapsules were obtained. SEM images of air-dried capsules show their intact and porous structures (Figure 3a,b). Confocal laser-scanning microscopy (CLSM) images (Figure 3c,d) show that unlike conventional PSS/PAH[14] and our PFS^-/PFS^+[5] capsules, DNA/PFS microcapsules display complete permeability for large molecules (Figure 3c) and macromolecules (Figure 3d). The unusual permeability behavior is believed to originate in the unique macroporous structures of the as-prepared capsule walls.

As mentioned earlier, the redox-active component PFS makes the obtained DNA/PFS macroporous structures responsive to chemical oxidation. A quartz crystal microbalance (QCM) was used to follow the thin-film oxidation process upon exposure to aqueous ferric chloride ($FeCl_3$) solutions. The recorded QCM frequency changes with time were converted to mass loss and are presented in Figure 4a. In contrast to other PFS-containing multilayer systems that bear

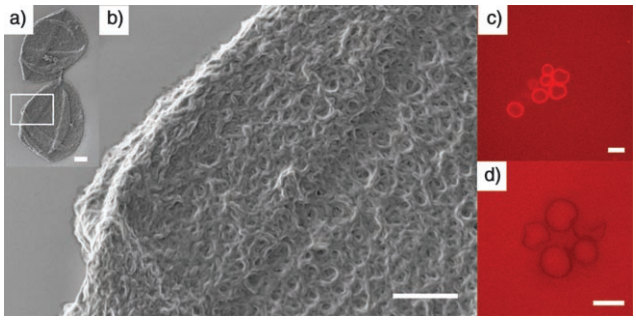

Figure 3. $(DNA/PFS)_5$ microcapsules: SEM images of a) collapsed air-dried $(DNA/PFS)_5$ microcapsules (scale bar is 2 μm) and b) porous capsule wall with a high magnification from the square zone in (a) (scale bar is 1 μm). CLSM images of $(DNA/PFS)_5$ microcapsules in the presence of c) TRITC-dextran (6.6×10^4 g mol^{-1}, hydrodynamic radius 9 nm[14]) and d) methacroyloxyethyl thiocarbamoyl rhodamine B (MRho) labelled PSS (1.2×10^5 g mol^{-1});[15] scale bars are 10 μm. All capsules display severe aggregation and excellent permeability for the probe molecules. Because of the different nature of the probe molecules, accumulation of TRITC-dextran and expulsion of anionic MRho-PSS were observed on the capsule wall.

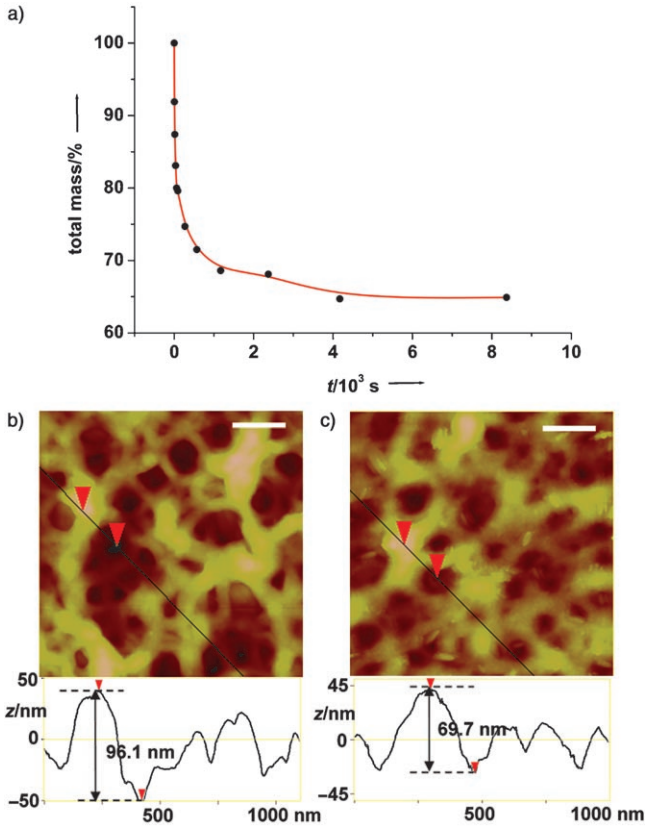

Figure 4. Oxidation of $PEI(DNA/PFS)_{10}$ thin films: a) Change in QCM frequency converted to mass loss with time by exposure to aqueous $FeCl_3$ solutions (1 mM, pH 4) on a QCM electrode. Sectional analysis of TM-AFM height images of b) as prepared, and c) after oxidation for five minutes by $FeCl_3$ (3 mM, pH 4); z range is 100 nm, scale bar is 200 nm for both images. A decrease in height of the ridges relative to the voids was observed.

a continuous thin-film morphology, DNA/PFS thin films did not disintegrate completely upon oxidation. However, a fast material loss of up to 35% of the total mass of the as-prepared thin film was obtained. We speculate this to be the result of a partial release of the PFS species in order to maintain charge neutrality of the network structure, as PFS becomes more positively charged after oxidation. Since an estimated total weight loss of 45% was expected for the full oxidation of PFS, the result shown in Figure 4a suggests incomplete oxidation. Although loss of material took place during chemical oxidation, AFM topography images showed that these films sustained their unique macroporous architectures (Figure 4b,c). Additionally, the height of the ridges relative to the voids, which could also be interpreted as the effective film thickness, decreased to ≈3/4 of its original value. Similarly, $(DNA/PFS)_5$ microcapsules exhibited high resistance to chemical oxidation. They kept their integrity in the presence of $FeCl_3$ (1 mM) for a rather long period (more than 24 h), while $(PFS^-/PFS^+)_5$ microcapsules disintegrated within 30 minutes under the same experimental conditions.[5]

In summary, we have demonstrated the successful electrostatic layer-by-layer self-assembly of high-molar-mass double-stranded DNA and PFS polycations into thin films and microcapsules bearing three-dimensional macroporous struc-

tures. It is believed that the formation of the highly porous architectures largely originates in the persistence length and chain-length mismatch of the two components, as well as the hydrophobicity of the PFS backbone. These porous structures may have potential applications in new cell scaffold materials, gene therapy, biocompatible surfaces, and controlled, active, molecular release systems.

Experimental Section

Materials: Poly(ethyleneimine) (PEI, $M_w = 2.5 \times 10^4\ g\,mol^{-1}$), deoxyribonucleic acid sodium salt from salmon testes (DNA, $M_w = 1.3 \times 10^6\ g\,mol^{-1}$, $\approx$2000 bp) were obtained from Sigma-Aldrich and used as received. The synthesis of PFS polycations (PFS^+, $M_w = 5.3 \times 10^4\ g\,mol^{-1}$) was described elsewhere.[7] The molar mass of PFS^+ was estimated on the basis of the repeat-unit molar mass and the average degree of polymerization obtained from GPC of the precursor polymer (poly[ferrocenyl(3-iodopropyl)methylsilane]) in THF, relative to PS standards.

LBL thin-film fabrication: After a standard cleaning procedure,[9b] quartz slides, silicon wafers, or QCM electrode substrates were first dipped into a PEI solution (about 10 mM) for 30 minutes to impart positively charged surfaces. Then the modified substrates were alternatively dipped in the PFS polycation and DNA aqueous solutions (2 $mg\,mL^{-1}$, 0.5 M NaCl) for 10 minutes, with rinsing, dipping into pure MilliQ, a second rinsing, and drying with a stream of nitrogen between each deposition step.

LBL microcapsule fabrication: Alternating adsorption of polyelectrolytes (1 $mg\,mL^{-1}$) onto $MnCO_3$ microparticles (average diameter 10 μm, about 10% w/w in suspension) was carried out in 0.5 M NaCl solution for 10 min followed by centrifugation (1000 rpm, 2 min) and three washing/centrifugation steps with MilliQ water. After depositing the desired number of polyelectrolyte bilayers, the templates were dissolved by using 0.2 M EDTA (pH 7) solution. The resultant capsules were washed thoroughly with and resuspended in MilliQ water.

Oxidation: Thin films were oxidized by immersion into $FeCl_3$ solution (1–3 mM, pH 4) for desired time intervals, then rinsed thoroughly with MilliQ water and dried under a stream of nitrogen.

Characterization: AFM experiments were performed using a NanoScope IIIa multimode AFM (Veeco-Digital Instruments, Santa Barbara, CA) in tapping mode with silicon cantilevers (Nanosensors, Wetzlar, Germany) at room temperature in air or in a liquid cell. For SEM images, thin-film or air-dried capsule samples were examined with a high-resolution LEO 1550 FEG SEM at acceleration voltages of 2.5 kV. CLSM images were taken with a Zeiss LSM 510 (63× oil immersion objective) system. Equal volumes of capsule suspension and fluorescence probe were mixed before observation.

Received: October 9, 2006
Published online: January 25, 2007

Keywords: DNA · polyelectrolytes · porosity · redox chemistry · self-assembly

[1] a) A. G. Mikos, A. J. Thorsen, L. A. Czerwonka, Y. Bao, R. Langer, D. N. Winslow, J. P. Vacanti, *Polymer* **1994**, *35*, 1068–1077; b) A. Imhof, D. J. Pine, *Nature* **1997**, *389*, 948–951; c) B. T. Holland, C. F. Blanford, T. Do, A. Stein, *Chem. Mater.* **1999**, *11*, 795–805; d) T. Nishikawa, R. Ookura, J. Nishida, K. Arai, J. Hayashi, N. Kurono, T. Sawadaishi, M. Hara, M. Shimomura, *Langmuir* **2002**, *18*, 5734–5740; e) J. L. Blin, A. Leonard, Z. Y. Yuan, L. Gigot, A. Vantomme, A. K. Cheetham, B. L. Su, *Angew. Chem.* **2003**, *115*, 2978–2981; *Angew. Chem. Int. Ed.* **2003**, *42*, 2872–2875; f) A. Collins, D. Carriazo, S. A. Davis, S. Mann, *Chem. Commun.* **2004**, 568–569; g) V. J. Chen, P. X. Ma, *Biomaterials* **2004**, *25*, 2065–2073; h) Y. F. Liu, S. P. Wang, J. W. Lee, N. A. Kotov, *Chem. Mater.* **2005**, *17*, 4918–4924; i) X. Roy, P. Sarazin, B. D. Favis, *Adv. Mater.* **2006**, *18*, 1015–1019.

[2] Reviews: a) O. D. Velev, E. W. Kaler, *Adv. Mater.* **2000**, *12*, 531–534; b) U. H. F. Bunz, *Adv. Mater.* **2006**, *18*, 973–989.

[3] a) J. D. Mendelsohn, C. J. Barrett, V. V. Chan, A. J. Pal, A. M. Mayes, M. F. Rubner, *Langmuir* **2000**, *16*, 5017–5023; b) M. C. Berg, L. Zhai, R. E. Cohen, M. F. Rubner, *Biomacromolecules* **2006**, *7*, 357–364.

[4] a) G. Decher, *Science* **1997**, *277*, 1232–1237; b) E. Donath, G. B. Sukhorukov, F. Caruso, S. A. Davis, H. Möhwald, *Angew. Chem.* **1998**, *110*, 2324–2327; *Angew. Chem. Int. Ed.* **1998**, *37*, 2202–2205; c) J. Hiller, J. D. Mendelsohn, M. F. Rubner, *Nat. Mater.* **2002**, *1*, 59–63; d) Z. Y. Tang, N. A. Kotov, S. Magonov, B. Ozturk, *Nat. Mater.* **2003**, *2*, 413–418.

[5] Y. Ma, W. F. Dong, M. A. Hempenius, H. Möhwald, G. J. Vancso, *Nat. Mater.* **2006**, *5*, 724–729.

[6] P. J. Yoo, K. T. Nam, J. F. Qi, S.-K. Lee, J. Park, A. M. Belcher, P. T. Hammond, *Nat. Mater.* **2006**, *5*, 234–240.

[7] a) M. A. Hempenius, N. S. Robins, M. Péter, E. S. Kooij, G. J. Vancso, *Langmuir* **2002**, *18*, 7629–7634; b) M. A. Hempenius, G. J. Vancso, *Macromolecules* **2002**, *35*, 2445–2447; c) M. A. Hempenius, F. F. Brito, G. J. Vancso, *Macromolecules* **2003**, *36*, 6683–6688; d) M. Ginzburg, J. Galloro, F. Jäkle, K. N. Power-Billard, S. Yang, I. Sokolov, C. N. C. Lam, A. W. Neumann, I. Manners, G. A. Ozin, *Langmuir* **2000**, *16*, 9609–9614; e) J. Halfyard, J. Galloro, M. Ginzburg, Z. Wang, N. Coombs, I. Manners, G. A. Ozin, *Chem. Commun.* **2002**, 1746–1747; f) K. N. Power-Billard, I. Manners, *Macromolecules* **2000**, *33*, 26–31; g) Z. Wang, A. Lough, I. Manners, *Macromolecules* **2002**, *35*, 7669–7677.

[8] I. Manners in *Synthetic Metal-Containing Polymers*, Wiley-VCH, Weinheim, **2004**.

[9] a) M. T. Nguyen, A. F. Diaz, V. V. Dement′ev, K. H. Pannell, *Chem. Mater.* **1993**, *5*, 1389–1394; b) M. Péter, M. A. Hempenius, E. S. Kooij, T. A. Jenkins, S. J. Roser, W. Knoll, G. J. Vancso, *Langmuir* **2004**, *20*, 891–897; c) S. Zou, M. A. Hempenius, H. Schönherr, G. J. Vancso, *Macromol. Rapid Commun.* **2006**, *27*, 103–108.

[10] a) Z. Xiao, M. Xu, K. Sagisaka, D. Fujita, *Thin Solid Films* **2003**, *438–439*, 114–117; b) T. Kanno, H. Tanaka, N. Miyoshi, T. Kawai, *Appl. Phys. Lett.* **2000**, *77*, 3848–3850.

[11] R. Rulkens, A. J. Lough, I. Manners, S. R. Lovelace, C. Grant, W. E. Geiger, *J. Am. Chem. Soc.* **1996**, *118*, 12683–12695; the persistence length was estimated from the molecular structure and X-ray diffraction studies of the polymer.

[12] a) G. Maurstad, S. Danielsen, B. T. Stokke, *J. Phys. Chem. B* **2003**, *107*, 8172–8180; b) C. G. Baumann, S. B. Smith, V. A. Bloomfield, C. Bustamante, *Proc. Natl. Acad. Sci. USA* **1997**, *94*, 6185–6190; c) J. R. Wenner, M. C. Williams, I. Rouzina, V. A. Bloomfield, *Biophys. J.* **2002**, *82*, 3160–3169.

[13] a) O. I. Vinogradova, O. V. Lebedeva, K. Vasilev, H. Gong, J. Garcia-Turiel, B.-S. Kim, *Biomacromolecules* **2005**, *6*, 1495–1502; b) H. Gong, J. Garcia-Turiel, K. Vasilev, O. I. Vinogradova, *Langmuir* **2005**, *21*, 7545–7550.

[14] W.-F. Dong, J. K. Ferri, T. Adalsteinsson, M. Schönhoff, G. B. Sukhorukov, H. Möhwald, *Chem. Mater.* **2005**, *17*, 2603–2611.

[15] L. Dähne, S. Leporatti, E. Donath, H. Möhwald, *J. Am. Chem. Soc.* **2001**, *123*, 5431–5436.

